

Article

Phosphorous Supply to a Eutrophic Artificial Lake: Sedimentary versus Groundwater Sources

Wiebe Förster ^{1,*}, Jan C. Scholten ^{1,*}, Michael Schubert ², Kay Knoeller ², Nikolaus Classen ³, Michael Lechelt ⁴, Jan-Helge Richard ⁴, Udo Rohweder ⁴, Isabell Zunker ⁴ and Susanne C. Wanner ⁴

¹ Institute of Geosciences, University Kiel, Otto-Hahn-Platz 1, 24118 Kiel, Germany; wiebe.foerster@yahoo.de

² UFZ—Helmholtz Centre for Environmental Research, Permoserstr. 15, 04318 Leipzig, Germany; michael.schubert@ufz.de (M.S.); kay.knoeller@ufz.de (K.K.)

³ Behörde für Umwelt, Klima, Energie und Agrarwirtschaft, Freie und Hansestadt Hamburg, Neuenfelder Str. 19, 21109 Hamburg, Germany; nikolaus.classen@bukea.hamburg.de

⁴ Institut für Hygiene und Umwelt, Freie und Hansestadt Hamburg, Marckmannstr. 129A, 20539 Hamburg, Germany; michael.lechelt@hu.hamburg.de (M.L.); jan-helge.richard@hu.hamburg.de (J.-H.R.); udo.rohweder@hu.hamburg.de (U.R.); isabell.zunker@hu.hamburg.de (I.Z.); wanner@wtnet.de (S.C.W.)

* Correspondence: jan.scholten@ifg.uni-kiel.de



Citation: Förster, W.; Scholten, J.C.; Schubert, M.; Knoeller, K.; Classen, N.; Lechelt, M.; Richard, J.-H.; Rohweder, U.; Zunker, I.; Wanner, S.C. Phosphorous Supply to a Eutrophic Artificial Lake: Sedimentary versus Groundwater Sources. *Water* **2021**, *13*, 563. <https://doi.org/10.3390/w13040563>

Academic Editor: Sotiris Orfanidis

Received: 17 December 2020

Accepted: 18 February 2021

Published: 23 February 2021

Publisher's Note: MDPI stays neutral with regard to jurisdictional claims in published maps and institutional affiliations.



Copyright: © 2021 by the authors. Licensee MDPI, Basel, Switzerland. This article is an open access article distributed under the terms and conditions of the Creative Commons Attribution (CC BY) license (<https://creativecommons.org/licenses/by/4.0/>).

Abstract: The eutrophic Lake Eichbaumsee, a ~1 km long and 280 m wide (maximum water depth 16 m) dredging lake southeast of Hamburg (Germany), has been treated for water quality improvements using various techniques (i.e., aeration plants, removal of dissolved phosphorous by aluminum phosphorous precipitation, and by Bentophos[®] (Phoslock Environmental Technologies, Sydney, Australia), adsorption) during the past ~15 years. Despite these treatments, no long-term improvement of the water quality has been observed and the lake water phosphorous content has continued to increase by e.g., ~670 kg phosphorous between autumn 2014 and autumn 2019. As no creeks or rivers drain into the lake and hydrological groundwater models do not suggest any major groundwater discharge into the lake, sources of phosphorous (and other nutrients) are unknown. We investigated the phosphorous fluxes from sediment pore water and from groundwater in the water body of the lake. Sediment pore water was extracted from sediment cores recovered by divers in August 2018 and February 2019. Diffusive phosphorous fluxes from pore water were calculated based on phosphorus gradients. Stable water isotopes ($\delta^2\text{H}$, $\delta^{18}\text{O}$) were measured in the lake water, in interstitial waters in the banks surrounding the lake, in the Elbe River, and in three groundwater wells close to the lake. Stable isotope ($\delta^2\text{H}$, $\delta^{18}\text{O}$) water mass balance models were used to compute water inflow/outflow to/from the lake. Our results revealed pore-water borne phosphorous fluxes between 0.2 mg/m²/d and 1.9 mg/m²/d. Assuming that the measured phosphorous fluxes are temporarily and spatially representative for the whole lake, about 11 kg/a to 110 kg/a of phosphorous is released from sediments. This amount is lower than the observed lake water phosphorous increase of ~344 kg between April 2018 and November 2018. Water stable isotope ($\delta^2\text{H}$, $\delta^{18}\text{O}$) compositions indicate a water exchange between an aquifer and the lake water. Based on stable isotope mass balances we estimated an inflow of phosphorous from the aquifer to the lake of between ~150 kg/a and ~390 kg/a. This result suggests that groundwater-borne phosphorous is a significant phosphorous source for the Eichbaumsee and highlights the importance of groundwater for lake water phosphorous balances.

Keywords: lake water/groundwater interaction; stable isotopes; phosphorous; eutrophication

1. Introduction

Eutrophication is one of the main reasons for the poor ecological status of many lakes around the world, causing the deterioration of lake water quality and occurrences of harmful cyanobacteria blooms [1,2]. High nutrient (i.e., phosphorus and nitrogen) supply via river and groundwater discharge or (to a minor degree) by atmospheric deposition are

pathways potentially leading to lake eutrophication [3,4]. A further lake nutrient source is related to the internal recycling of nutrients from lake sediments [5–7]. The term “internal recycling” describes the fixation of nutrients in sediments during the full circulation of the lake’s water body usually during winter and their release from the sediments (via sediment pore water diffusion) during lake water stagnation usually during summer. Many of these release processes are sensitive to both oxygen contents as well as the temperature of water and sediments with elevated nutrient release rates under anoxic and/or warm conditions [8].

Whereas nutrient sources of rivers and creeks can be determined relatively easily, e.g., by measuring river water fluxes and their nutrient concentrations, groundwater-borne nutrient supply is more difficult to quantify and, as some studies suggested, may be not relevant for lake water nutrient budgets at all [9]. However, there is growing evidence that groundwater discharge (i.e., the flow of groundwater to a lake) and lake water exfiltration into the aquifer (i.e., water flow from the lake to the groundwater) are important processes influencing the nutrient budgets of lakes [10–12]. For instance, Kazmierczak et al. [13] showed recently the importance of groundwater enriched in phosphorus in sustaining the eutrophic level of a 0.16 km² shallow lake in Denmark. Determining such water flux to or from a lake water body may be difficult to quantify especially in cases where a hydraulic connection between lake and aquifer is not obvious from e.g., hydrological maps or models.

Water stable isotope signatures of oxygen and hydrogen ($\delta^2\text{H}$ and $\delta^{18}\text{O}$, i.e., D/O) are useful tracers for investigating groundwater-lake water interactions [14–17]. These ratios are characteristic for various water types, which differ in their isotopic composition (i.e., their D/O signature) due to isotopic fractionation during evaporation. Based on a D/O mass balance, which considers the inflow of water to the lake (groundwater discharge, precipitation) as well as the outflow (lake water exfiltration, evaporation), quantitative estimates of the groundwater/lake water interactions can be derived [16], which in turn can be used to estimate groundwater-borne solute fluxes into the lake [17].

Poor lake water quality requires remediation measures that aim at the reduction of lake water external and internal nutrient (i.e., nitrogen and phosphorus) loads [18]. It has to be kept in mind, though, that the response time of lakes, when reducing external inputs by e.g., reducing fertilizer usage and/or reducing waste water disposal, may result in time lags of several decades before a lower eutrophication level is achieved [19]. Furthermore, it has to be considered that a reduction of nitrogen alone is not sufficient to improve water quality [20]. While a reduction of a lake’s nitrogen concentrations would lead to a lower nitrogen/phosphorus (N/P) ratio, which is generally unfavorable for most algae, nitrogen fixers such as cyanobacteria can bind nitrogen from the atmosphere in order to maintain the required N/P ratio [21]. Thus, nitrogen limitation alone will maintain high biomass growth and excessive growth of cyanobacteria causing poor water quality potentially endangering people’s health [1,22].

Reducing phosphorus is now widely accepted to be the most important factor controlling the eutrophication of lakes [20]. As internal cycling continuously replenishes the lake water phosphorus inventory, dredging of phosphorus-rich surface sediments has been proposed as an appropriate lake remediation measure [23]. However, dredging the lake and transferring the sediment to a disposal site is quite costly. Another approach is to increase the sediment’s sorption capacity for phosphorus by adding alum (basically aluminum sulfate) or by adding lanthanum [24–27], which is a more cost-effective remediation measure. Alternatively, the lake can be artificially aerated to prevent anaerobic bottom water conditions, which aims at reducing internal phosphorus cycling.

Only 14 years after its formation in 1976 Lake Eichbaumsee, an artificial lake southeast of Hamburg (Germany) (Figure 1), showed elevated nutrient concentrations demanding remediation measures. In November 2003 phosphorous removal from the water column using aluminum-sulfate did not reduce phosphorous effectively. Further installations of sub water surface aeration devices in 2005 and 2007 that forced water column circulation as well as the aeration of the lake’s deep water did not stop the increase of phosphorous in the water

body (Figure 2). Further lake water treatments using Bentophos[®] (a lanthanum-modified bentonite; Bentophos[®]) were applied, which are expected to bind and fix phosphorous permanently in the sediments. Each November between 2010 and 2013 Bentophos[®] was added to the lake (288 t in total) [28]. The Bentophos[®] treatments in November 2010 and 2013 removed about 90% of the phosphorous from the water column (Figure 2). After the last Bentophos[®] application it was decided by the local authorities that no further treatments would be necessary [28]. However, in 2014 phosphorous increased by 306 kg between spring and autumn with little reduction during full water column circulation in the following winter 2015 (Figure 2). Since then, lake water phosphorus concentrations and eutrophication levels remained high triggering harmful algal blooms regularly during the spring and summer [29].



Figure 1. Location of Eichbaumsee close to Hamburg; E2, E3, and E4 indicate water column and sediment core sampling locations; P1–P6, Pc, and Pb are the push-point sampling locations; DE indicates the Dove-Elbe sampling location; GW979, GW5028, and GW11028 indicate the locations of groundwater wells; Brack is a small lake north of Eichbaumsee (Source of images: GeoFly.de, and Google Earth).

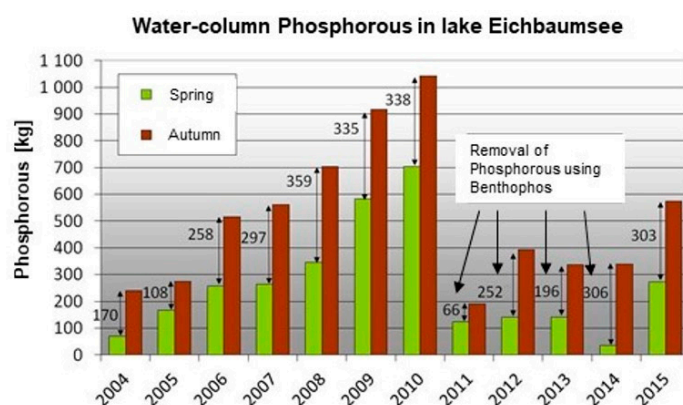


Figure 2. Phosphorous content of Lake Eichbaumsee in spring and autumn between 2004 and 2015. Numbers with arrows indicate the phosphorous increase (kg) between spring and autumn. The application of Bentophos[®] in the winters 2011 through 2013 did not lead to a long-term reduction of the lake phosphorous content (modified from [28]).

These unsuccessful remediation attempts have raised the question as to whether the lake phosphorous increase is related to the failure of Bentophos[®] to fix phosphorous in the sediments permanently or if an additional and so far unconsidered external phosphorous source exists. As no creeks or rivers discharge into the lake and available hydrological groundwater models do not suggest any major groundwater flow into the lake, the nature of any such external phosphorous source remained unknown.

In our study we investigated the internal and external phosphorous supply to Lake Eichbaumsee using sediment geochemistry and sediment-porewater flux measurements to quantify the internal phosphorous source. Based on water stable isotope mass balances we discuss a groundwater-borne phosphorous supply. To our knowledge this is the first study combining such methodological approaches to constrain a lake phosphorous balance. Our results reveal that, apart from the internal phosphorous cycling, groundwater-borne phosphorous is a very important source for the overall phosphorous budget of the lake maintaining its eutrophication level. This result highlights the importance of recognizing groundwater as a phosphorous source before lake water remediation measures are designed.

2. Methods

2.1. Study Area

Lake Eichbaumsee is located southeast of Hamburg (Figure 1) in the North German sedimentary plain. During several Quaternary glaciations/deglaciation periods meltwaters formed the River Elbe valley and deposited a wide range of glacial sediments (sands, tills, gravels). Below a ~5–10 m thick clayey layer ~25–30 m thick Holocene sands were deposited. Extractions of these sands for road constructions in 1972–1976 formed the Lake Eichbaumsee. The artificial lake is max. 1 km long and 280 m wide with an average depth of 6.5 m and a maximum depth of 16 m. The lake's surface area is 240,000 m² and the water volume is around 1,727,000 m³ [28]. The lake used to be directly connected to a branch of River Elbe, the so-called Dove-Elbe, until its straightening in 1977. No creeks drain into the lake. To the north of the lake an east-west trending dyke (Moorfleeter Deich, Figure 1) was constructed in the 19th century to protect the hinterland with farming land from possible flooding of the Elbe River. Two natural reserves border the Eichbaumsee to the east and to the south. The lake has an important function as a local recreation area and as the lake is used for swimming, water quality has been monitored regularly throughout the years by local authorities.

2.2. Sampling Locations

Three sampling campaigns were carried out: 10–11 April 2018, 14–15 August 2018, and 26–27 February 2019. During these campaigns, sediments, sediment pore waters, ground water samples, lake water column samples, as well as pore water samples from the lake banks were collected. An overview of the sampling and sampling locations is given in Figure 1 and Table 1.

Table 1. Sample types, sampling campaigns, and locations.

Sample Type	Date	Locations
Sediments	April	E2, E3, E4
Sediment pore water	April	E2, E4
Sediment pore water	August 2018, February 2019	E2, E4
Push-point samples	August 2018, February 2019	P1–P6; Pb, Pc
Groundwater	April 2018, February 2019	GW 11028, GW 5028, GW 979
Water column	April 2018, May 2018, July 2018, August 2018, November 2018, February 2019	E2, E4 (only April, August, February)
Dove-Elbe	April 2018, August 2018, February 2019	DE

2.2.1. Sediment and Sediment Pore Water Sampling

Three deep locations in the lake (E2: 14 m, E3: 13 m, and E: 16 m) were selected as coring stations because the highest accumulation of soft sediments was expected here, a situation that is favorable for sediment core recovery by divers who pushed PVC liners (with lengths between 0.5–1 m, diameter 10 cm) into the soft lake sediment. Upon recovery,

sediment pore water was collected from the cores by pushing Rhizons into pre-drilled holes in the liner (intervals between 1 and 2 cm) and extracting pore water following the procedure given in Seeberg-Elverfeldt et al. [30]. For analysis of major and minor ions one fraction of pore water was immediately acidified with HNO₃ in order to prevent the formation of hydrous ferric oxides and potential co-precipitation/sorption. A second fraction was stored in a freezer for later nutrient analyses. Furthermore, 2 mL of pore water was sampled in glass vials for water stable isotope analyses (D/O). Due to a failure in the preservation of pore water samples during the April campaign, we only report pore water data from August and February. In April, after pore-water sampling, sediments were extruded from the core and sampled in 1–5 cm thick slices for geochemical analyses.

2.2.2. Push-Point Sampling

From the lake banks pore water samples were obtained from 0.5–1.8 m depths using a push-point sampler [31]. The water samples were 0.45 µm filtered and separated in aliquots similar to the sediment pore water samples (see Section 2.2.1).

2.2.3. Lake Water and Groundwater Sampling

Lake water sampling for the chemical and physical characterization of the lake water body was conducted as full water-column profile sampling. Water temperature and oxygen content were determined using in situ sensors (EXO multiparameter sonde, YSI, Yellow Springs, OH, USA). Water samples were obtained in 0.3 m, 3 m, 6 m, 9 m, and 12 m water depths using Niskin[®] bottles.

The area of Hamburg hosts one of the most productive groundwater reserves in Europe with six main aquifers found in Quaternary to Tertiary sediments. The deepest aquifer (~500 m depth below surface) is found in sandy layers (Braunkohlesande), whereas the shallowest aquifer sits 2–5 m below surface in sandy Weichsel sediments. Groundwater samples were taken from three wells located in the vicinity of the lake. The wells GW979 and GW5028 tap water from Weichsel sandy sediments, whereas GW11028 waters are from sandy-silty sediments of the Saale age. The respective groundwater levels sit between 0.8 m and 0.2 m above sea-level with seasonal fluctuations of less than 0.5 m (note that the Lake Eichbaumsee level is ~0.5 m above sea-level). All groundwater samples were obtained after purging the wells for about 15 min until water conductivity remained constant. The samples were 0.45 µm filtered, and aliquots for major and minor element analyses, nutrients, and stable isotopes (D/O) were obtained following the procedure outlined above (see Section 2.2.1).

2.3. Chemical Analyses

2.3.1. Water Samples

Phosphorous in water samples was analyzed as ortho-phosphate (PO₄³⁻) using continuous flow analysis (CFA) (Allianz Instruments). Phosphorus, iron, manganese, and lanthanum analyses in all water samples were performed using an Agilent 8800 ICP-MS/MS in mass-shift-mode (m/z 31 → m/z 47) after reaction with O₂ to avoid ¹⁴N¹⁶OH⁺-interferences. Accuracy was checked by analyzing phosphorous and iron standard solutions (Merck KGaA). The precisions ranged between ±10% (ICP-MS) and ±20% (CFA).

2.3.2. Major Elements in Sediments

For the analyses of major elements (Si, Al, Fe, Mn, Mg, Ca, K, Ti, P) about 200 mg of ground sediments were dissolved in a mixture of HNO₃, HCl, and HF. Measurements were conducted in the presence of an yttrium internal standard using ICP-OES (Inductively Coupled Plasma Optical Emission Spectrometry, SPECTRO Ciros). For measurements of lanthanum (La) we used a Quadrupole ICP-MS (Agilent 7500 cc) with an Octopole reaction system. For the quality control of the measurements three sediment/rock standards (GSMS-2; BHVO_2, BIR_1a) were used. The analytical precision was ≤2%. In order to correct for

the loss of silica during sample preparation, loss on ignition was determined by weighing sediment samples before and after heating to 1000 °C.

2.3.3. Stable Isotope Analyses

Water stable isotope analyses were carried out using laser cavity ring-down spectroscopy (Picarro L2120-i, Santa Clara, CA, USA). The results of the hydrogen and oxygen isotope measurements are expressed as delta notations ($\delta^2\text{H}$, $\delta^{18}\text{O}$) relative to the Vienna standard mean ocean water (VSMOW). The analytical uncertainties of $\delta^{18}\text{O}$ and $\delta^2\text{H}$ measurements are $\pm 0.1\text{‰}$ and $\pm 0.8\text{‰}$, respectively.

2.4. Calculation of Pore Water Fluxes

Diffusive phosphorous fluxes from the sediment pore water to the overlying lake water were calculated following first Fick's law [32] where F is diffusive flux, n is the sediment porosity (-), D_s is the diffusion coefficient ($\text{cm}^2 \text{s}^{-1}$), and $\frac{\partial C}{\partial x}$ is the concentration gradient (mg cm^{-2}). The porosity was determined from the sediment water content; the diffusion coefficient was calculated following Ullman & Aller [33].

$$F \left[\frac{\text{mg}}{\text{cm}^2 \text{s}} \right] = n \times D_s \times \frac{\partial C}{\partial x} \quad (1)$$

2.5. Water Stable Isotope Mass Balance

The determination of groundwater discharge into the lake based on a D/O mass balance assumes that the D/O signature of the lake water is controlled by (i) the physical lake water/groundwater interaction, (ii) precipitation, and (iii) evaporation [16,17], with δ_P , δ_{G_i} , δ_E , and δ_{G_o} (‰) being the isotopic signatures of precipitation (P (mm)), groundwater discharge (G_i ($\text{m}^3 \text{day}^{-1}$)), evaporation (E (mm)) and groundwater exfiltration (G_o ($\text{m}^3 \text{day}^{-1}$)), respectively. A constant lake volume (V (m^3)) over time is assumed. Furthermore, the isotopic signature of the lake water (δ_L) is assumed to be representative of the lake water that is exfiltrating into the aquifer (δ_{G_o}) [16].

$$P\delta_P + G_i\delta_{G_i} = E\delta_E + G_o\delta_{G_o} \quad (2)$$

The isotopic signature of the evaporate (δ_E) is given by [34],

$$\delta_E = \frac{\frac{\delta_{L_s} - \epsilon^+}{\alpha^+} - h \times \delta_A - \epsilon_K}{1 - h + 10^{-3} \times \epsilon_K} \quad (3)$$

with δ_{L_s} being the isotopic signature of the lake's surface water (‰), ϵ^+ the equilibrium isotopic separation (-), α^+ the equilibrium isotopic fraction factor (-), h the relative humidity (-), δ_A the isotopic composition of atmospheric moisture (‰), and ϵ_K the kinetic isotopic separation (‰). ϵ^+ was calculated following Gibson et al. [15]; α^+ was obtained from the empirical solution proposed by Horita & Wesolowski [35]; the equilibrium isotopic separation factors ϵ^+ and ϵ_K were calculated following Gonfiantini [36].

The isotopic composition of atmospheric moisture (δ_A) was determined based on δ_P , ϵ^+ , and the seasonality factor k (-) [15,16].

$$\delta_A = \frac{\delta_P - k \times \epsilon^+}{1 + 10^{-3} \times k \times \epsilon^+} \quad (4)$$

The seasonality factor accounts for the changes in the isotopic fractionation during evaporation in a seasonal cycle with $k = 0.5$ for strong seasonal climate alterations and $k = 1$ for climates with minor seasonality. Estimates of k are obtained by dual analysis of $\delta^{18}\text{O}$ and $\delta^2\text{H}$. A fit of the mean annual evaporation flux-weighted δ_A is adjusted by optimizing k to fit δ_E to the local evaporation line [37,38].

The remaining unknown parameter that has to be calculated to solve Equation (2) is the amount of groundwater discharging into the lake (G_i) as given by Knöller et al. [17] (Equation (5)):

$$G_i \left[\frac{\text{m}^3}{\text{day}} \right] = \frac{(S_i + P) \times \left(\frac{\delta_P}{\delta_L} - 1 \right) + E \times \left(1 - \frac{\delta_E}{\delta_L} \right)}{1 - \frac{\delta_G}{\delta_L}} \tag{5}$$

with S_i being surface water runoff (m^3). S_i was assumed to be the part of the precipitation that falls on the surroundings of the lake (i.e., the slope area around the lake) and subsequently drains into the lake [17]. A footpath around the lake was considered as the highest area around the lake, and the area between this path and the lake was chosen as the slope area for the S_i calculation.

3. Results

3.1. Water Column

Water column profiles of temperature and oxygen were obtained at locations E2 and E4 between April 2018 and February 2019 (Figures 3 and 4); phosphorous was measured at E2 only (Figure 5). Figure 3 illustrates that the lake water column is characterized by a well-developed thermocline during the summer months (May, July, and August) and a homogenous temperature distribution in the winter (November and February).

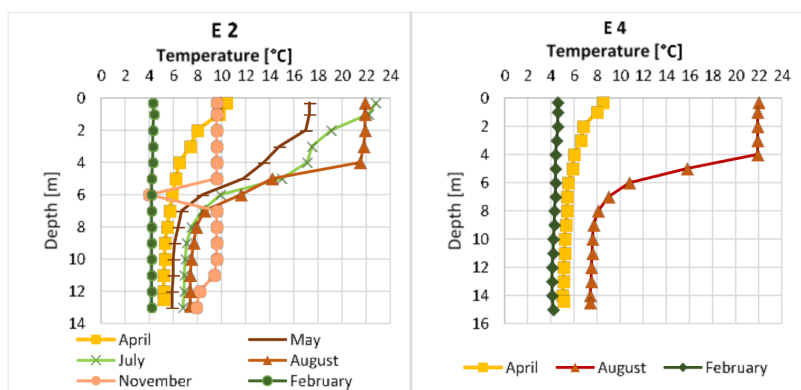


Figure 3. Temperature distribution in the water column of Lake Eichbaumsee at locations E2 and E4 between April 2018 and February 2019.

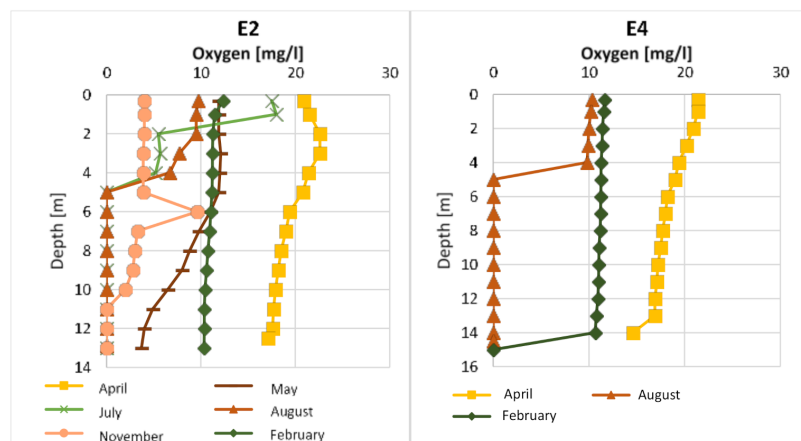


Figure 4. Oxygen distribution in the water column of Lake Eichbaumsee at locations E2 and E4 between April 2018 and February 2019.

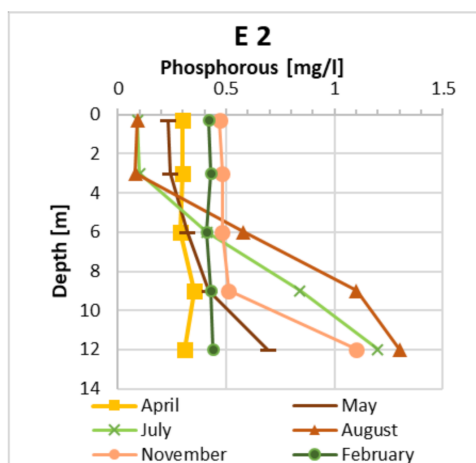


Figure 5. Phosphorous distribution in the water column of Lake Eichbaumsee at location E2 between April 2018 and February 2019.

Whereas oxygen was present throughout the water column in April, the water column below 6 m water depth was anoxic in July and August (Figure 4). In November, only the water column >10 m was still anoxic whereas in February oxygen was found throughout the water column. At location E4 with the greatest water depth (16 m) the water column >15 m was still anoxic in February.

Phosphorous concentrations in the water column were relatively constant ranging between 0.29 and 0.35 mg/L in April (Figure 5). In May the deep water (12 m) concentration increased to 0.69 mg/L. In July and August, a steep gradient developed between high phosphorous concentrations in deep waters (July: 1.20 mg/L; August: 1.30 mg/L) and low concentrations at 0.3 m, i.e., shallow water depth (July: 0.09 mg/L; August 0.09 mg/L). Whereas these high phosphorous concentrations were still present in November in deep water (1.10 mg/L at 12 m), in water depths ≤9 m phosphorous was found to be in a relatively small range (0.47–0.51 mg/L). A homogeneous phosphorous distribution (range 0.41–0.44 mg/L) throughout the water column was observed in February 2019.

The water column distributions of iron and manganese are characterized by seasonal changes comparable to those of phosphorous. In spring (April 2018, February 2019) both elements showed relatively low and constant concentrations (Figure 6). In May, July, and August, however, gradients between high deep-water and low mid-water concentrations were observed. Mixing of the water column caused homogenous distributions of iron and manganese in the water column at ≤9 m in November with elevated concentrations at a water depth of 12 m.

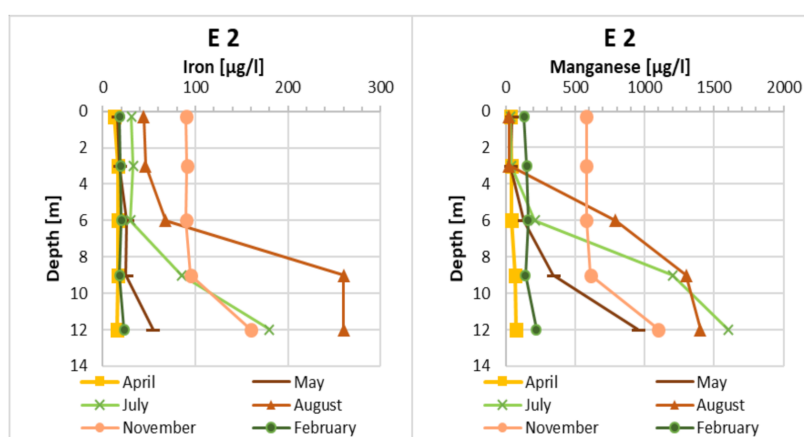


Figure 6. Iron and manganese distribution in the water column of Lake Eichbaumsee at location E2 between April 2018 and February 2019.

3.2. Phosphorous, Iron, and Lanthanum in Sediments

The obtained sediments consisted generally of homogeneous greyish-black silty mud. Sediments at the base of core E3 were composed of a light-greyish sand layer.

The results of the geochemical analyses of sediments can be found in the supplementary materials (Table S2).

Surface sediment phosphorous concentrations ranged between 1.75 g/kg (E4) and 3.79 g/kg (E2) (Figure 7). Maximum phosphorous concentrations were found in E2 at 2–3 cm depth (4.24 g/kg) and at 4–6 cm depth in E3 (3.24 g/kg). The concentrations decreased with increasing sediment depth to 0.87 g/kg (E2: 40–45 cm) and 0.41 g/kg (E3: 65.5–68 cm). In both cores we observed a general trend of increasing phosphorous concentrations with decreasing depths. For instance, in core E3 phosphorous concentrations increased by about a factor of seven (note that the base of this core consists of sandy sediments with ~90% SiO₂ content; cf. Table S2).

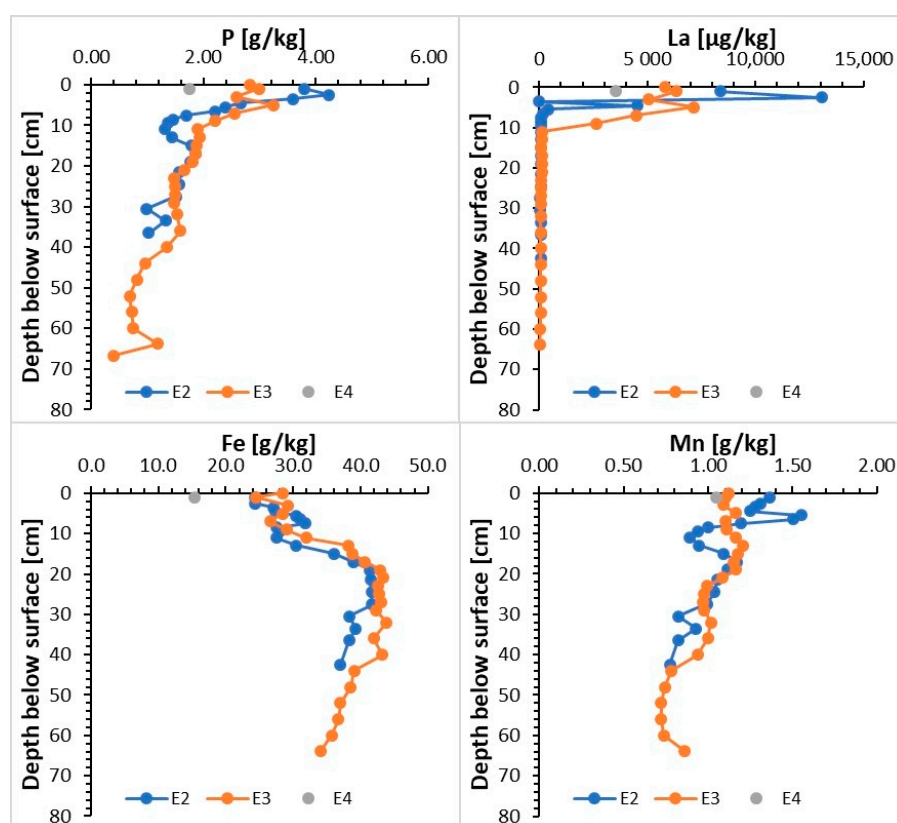


Figure 7. Distribution of phosphorous (P), lanthanum (La), iron (Fe), and manganese (Mn) in sediments cores E2, E3, and E4.

Lanthanum in surface sediments was highest in core E2 (8370 µg/g) and lowest in core E4 (3537 µg/g) (Figure 7). Concentration peaks were found at 2–3 cm (E2: 13,050 µg/g) and 4–6 cm (E2: 7160 µg/g), i.e., at the same depths as the maximum phosphorous concentrations. Below depths of 7–8 cm (E2) and 8–10 cm (E3) lanthanum concentrations ranged between 17 µg/g and 100 µg/g, respectively.

Iron concentrations at the sediment surface ranged between 15.3 g/kg (E4) and 28.4 g/kg (E3) and they increased steadily down to a sediment depth of about 18–20 cm (E2: 41.4 g/kg; E3: 42.9 g/kg) (Figure 7). In sediment depths of 20–30 cm (E2) and 20–42 cm (E3) concentrations remained relatively constant followed by a decrease with lowest values at the core base (E2: 40–45 cm: 37.0 g/kg; E3: 62–65.5 cm: 34.1 g/kg). Note that Fe was below the detection limit in the deepest sample of core E3.

Surface sediment manganese concentrations varied between 0.10 g/kg (E4) and 0.14 g/kg (E2) (Figure 7). In both cores the concentrations gradually decrease with increas-

ing sediment depth (E2: 0.05 g/kg at 65.5–68 cm; E3: 0.08 g/kg at 40–44 cm). In core E2 a subsurface manganese concentration maximum (0.15 g/kg) was detected at 5–6 cm.

The generally lower phosphorous, iron, manganese, and lanthanum concentrations in surface sediments at location E4 compared to E2 and E3 are probably related to higher SiO₂ concentrations in the E4 core causing a higher dilution of the other elements (Table S2).

3.3. Phosphorous Distribution in Sediment Pore Waters

As stated above, phosphorus was measured as ortho-phosphate via CFA and as total phosphorus via ICP-MS. The close relationship between ortho-phosphate (as P) and total phosphorus suggests that most of the phosphorus is bound as ortho-phosphate (Figure 8).

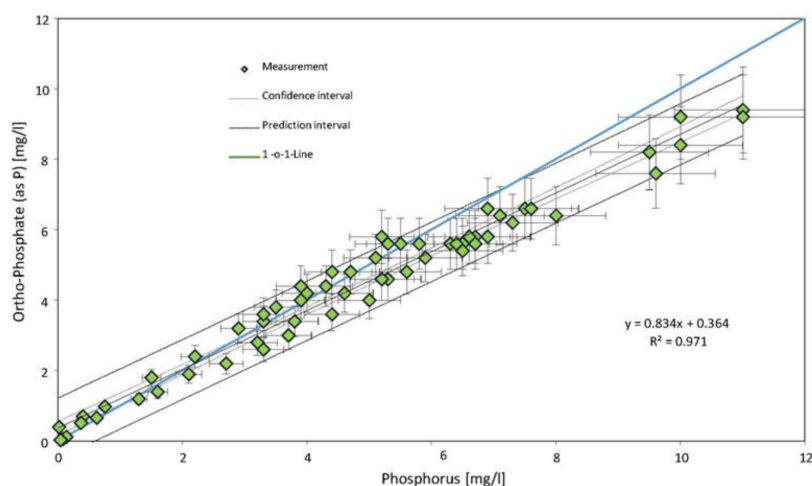


Figure 8. Relationship between ortho-phosphate (as P, measured by CFA) and total phosphorus (measured by ICP-MS) in sediment pore water samples in February 2019. The close relationship indicates that ortho-phosphate is the major phosphorus phase in sediment pore waters.

At locations E2 and E4 the sediment pore water phosphorous concentrations in August and February showed a gradient between low concentrations at the sediment/lake water interface (August E2: 0.63 mg/L; August E4: 1.80 mg/L; February E2: 0.40 mg/L; February E4: 0.37 mg/L) and a subsurface phosphorous maximum (August E2: 5.6 mg/L at 4 cm depth; August E4: 4.00 mg/L at 6 cm depth; February E2: 6.70 mg/L at 12 cm depth; February E4: 5.30 mg/L at 12 cm depth) (Figure 9). The diffusive phosphorous fluxes from sediment pore water (Equation (1)) ranged in August between 0.8 mg/m²/d (E2) and 1.9 mg/m²/d (E4) and between 0.2 mg/m²/d (E2) and 0.7 mg/m²/d (location E4) in February.

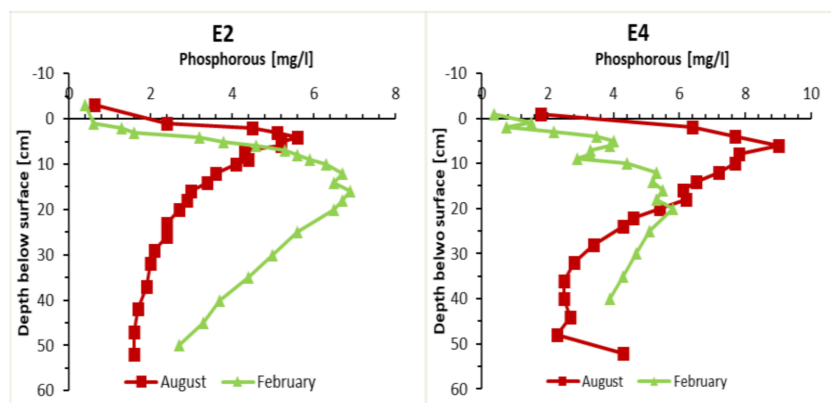


Figure 9. Phosphorous pore water profiles at locations E2 and E4 determined in August 2018 and 2019.

Both iron and manganese pore water profiles (Figure 10) are characterized by concentration gradients between low concentrations at the sediment/lake water interface (Fe: E2: August: 0.06 mg/L, February: 0.02 mg/L; E4: August: 0.18 mg/L, February: 0.03 mg/L) (Mn: E2: August: 1.10 mg/L, February: 0.46 mg/L; E4: August: 2.1 mg/L, February: 0.21 mg/L) and subsurface maxima (Fe: E2: August: 33.0 mg/L at 32 cm, February: 44.0 mg/L at 50 cm; E4: August: 34.0 mg/L at 32 cm; February: 26.0 mg/L at 40 cm) (Mn: E2: August: 5.9 mg/L at 4 cm, February: 8.5 mg/L at 12 cm; E4: August: 11.0 mg/L at 6 cm, February: 6.6 mg/L at 6 cm). In the upper part of the cores (~0–20 cm) the shape of the manganese and phosphorous concentration profiles are very similar (Figures 9 and 10).

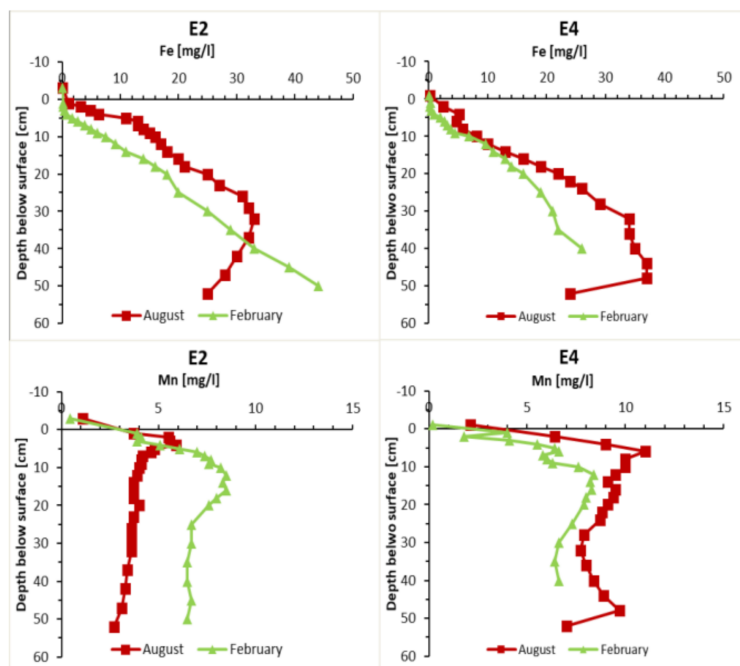


Figure 10. Iron (Fe) and manganese (Mn) pore water profiles at locations E2 and E4 determined in August 2018 and February 2019.

A peak in lanthanum pore water concentrations can be observed in February at locations E2 (7.40 $\mu\text{g/L}$ at 3 cm depth) and E4 (30 $\mu\text{g/L}$ at 1 cm depth) (Figure 11). The pore water profiles in August show only a slight enrichment of lanthanum at E2 (1 $\mu\text{g/L}$ at 1 cm and 2 cm depths) relative to the background concentrations (range ~0.01–0.5 $\mu\text{g/L}$) derived from deeper sediments. No pore water lanthanum peak was observed at E4 in August.

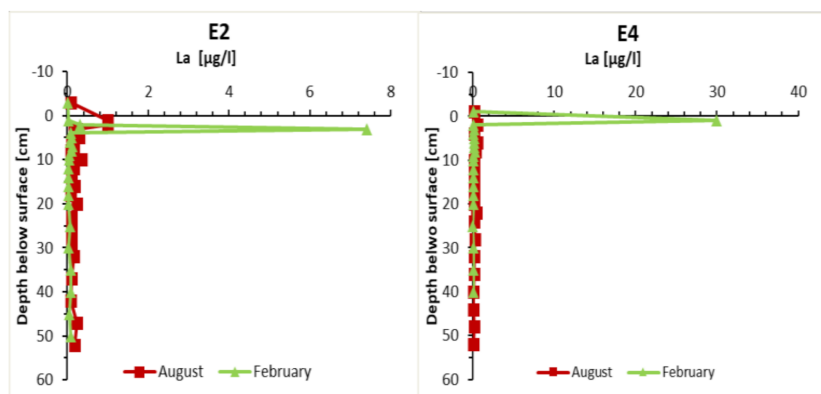


Figure 11. Lanthanum (La) pore water profiles at locations E2 and E4 determined in August 2018 and February 2019.

3.4. Phosphorous in Groundwater

The chemical composition of all groundwater samples taken from the wells is presented as supplementary material in Table S1. Phosphorous concentrations ranged between 0.42 mg/L (GW5028) and 0.70 mg/L in GW979 (Figure 12). Samples obtained from the banks of the lake by means of push-point sampling showed phosphorous concentrations between 0.34 mg/L and 0.70 mg/L. The Dove-Elbe river water showed phosphorous concentrations of 0.49 mg/L in August 2018 and 0.03 mg/L in February 2019 (note that no phosphorous data are available for April 2018) (Figure 12).

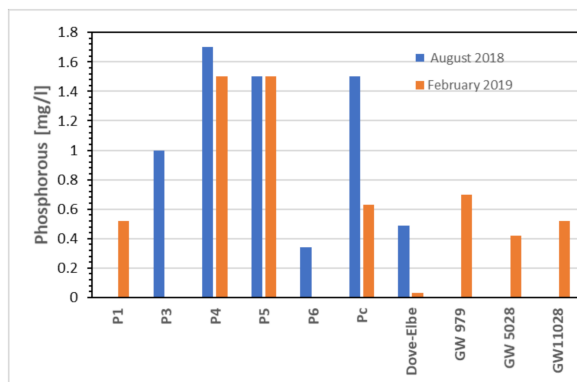


Figure 12. Phosphorous concentrations in push-point samples, the Dove-Elbe, and in groundwater.

3.5. Water Stable Isotopes

The isotopic signatures of water samples from the Dove-Elbe, from the wells GW11018 and GW5028, and the three push-point samples (P4, P5, P6) plot in the $\delta^{18}\text{O}/\delta^2\text{H}$ diagram close to both the Global Meteoric Water Line (GMWL, [39]) and Local Meteoric Water Line (LMWL, data from Global Network of Isotopes in Precipitation, location Cuxhaven) (Figure 13). These signatures differ from the isotopic signature of the lake water indicating that the lake is neither directly hydraulically connected to the Dove-Elbe nor to the groundwater represented by wells GW11028 and GW5028. Instead, the plot of the isotopic signature of the lake water is close to that of the groundwater sampled at well GW979. This suggests a water exchange between the aquifer and the lake in this area, i.e., at the northern bank of the lake. The quantification of this exchange will be discussed in the following based on a D/O mass balance (see Section 2.5, Equation (2)). The parameters of this mass balance are summarized in Table 2.

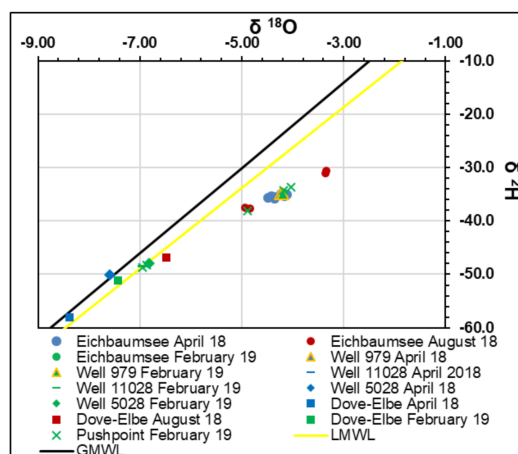


Figure 13. $\delta^{18}\text{O}$ and $\delta^2\text{H}$ of lake water, the Dove-Elbe, groundwater, and push-point samples, the global Meteoric Water Line (GMWL), and the Local Meteoric Water Line (LMWL). Lake water and groundwater from well 979 plot close to each other suggesting an exchange between this aquifer and the lake.

Table 2. Parameter used for solving the $\delta^{18}\text{O}$ and $\delta^2\text{H}$ mass balances.

Parameter	April 2018	August 2019	Unit
Lake surface area (S)	240,000	240,000	m ²
Lake water volume (V)	1,727,000	1,727,000	m ³
Precipitation (P)	8400	17,011	mm
Surface runoff (S _i)	2000	4050	m ³
Humidity (h)	0.72	0.72	(-)
Evaporation	16,200	29,940	mm
$\delta^{18}\text{O}$ Balance			
δ_P	-6.51	-6.64	‰
δ_L	-4.27	-3.88	‰
δ_{Ls}	-4.27	-3.35	‰
$\alpha+$	1.01	1.01	(-)
ϵ^+	10.8	10.0	(-)
ϵ_k	3.97	3.49	(-)
δ_A (k = 0.86)	-15.7	-15.7	‰
δ_A (k = 0.92)	-16.3	-16.3	‰
δ_E ($\delta_A = -15.7$)	-26.9	-21.0	‰
δ_E ($\delta_A = -16.3$)	-25.3	-17.3	‰
δ_G	-7.07	-7.07	‰
G _i	3800–4100	3600–4800	m ³ /d
G _o	3500–3800	3100–4200	m ³ /d
$\delta^2\text{H}$ Balance			
δ_P	-46.9	-45.1	‰
δ_L	-35.3	-30.5	‰
δ_{Ls}	-35.9	-32.9	‰
$\alpha+$	1.10	1.09	(-)
ϵ^+	97.9	87.2	(-)
ϵ_k	3.49	2.96	(-)
δ_A (k = 0.86)	-120	-112	‰
δ_A (k = 0.92)	-126	-116	‰
δ_E ($\delta_A = -120/-112$)	-125	-108	‰
δ_E ($\delta_A = -126/-116$)	-123	-94.5	‰
δ_G	-57.9	-57.9	‰
G _i	1900–2200	2100–2700	m ³ /d
G _o	1600–1900	1600–2200	m ³ /d

For solving Equation (2) we used meteorological data (precipitation, P (mm); air temperature, T (°C); and relative humidity, h (%); obtained from the German Weather Service weather station Fühlbüttel located 18 km from Lake Eichbaumsee), and the D/O signatures of the local precipitation (obtained from the GNIP (Global Network of Isotopes in Precipitation), www.iaea.org/services/networks/gnip (accessed on 16 December 2020); Cuxhaven, located about 100 km from Lake Eichbaumsee). Monthly D/O means were available for the years 1978 through 2012. Precipitation and evaporation (mm/d) were adapted to the surface area of the lake. The determination of the average isotopic signature of lake water (δ_L) was based on the depth weighted average isotopic water signatures determined in April (average of profiles E2 and E4: $\delta^{18}\text{O} = -4.28$ ‰; $\delta^2\text{H} = -35.3$ ‰) and in August ($\delta^{18}\text{O} = -3.88$ ‰; $\delta^2\text{H} = -32.9$ ‰). The lake surface water isotopic signature (δ_{Ls}) was obtained from surface water samples (April: $\delta^{18}\text{O} = -4.27$ ‰, $\delta^2\text{H} = -35.9$ ‰; August: $\delta^{18}\text{O} = -3.35$ ‰, $\delta^2\text{H} = -30.5$ ‰). The atmospheric moisture δ_A (Equation (4)) was determined following Petermann et al. [16] by varying the seasonality factor k to fit the local evaporation line (LEL) (Figure 14). The LEL was created based on lake water samples and the groundwater sample taken from well GW5028. The isotopic signature of δ_E ranges between -17.3 ‰ and -26.9 ‰ for $\delta^{18}\text{O}$ and between -94.5 ‰ and -116 ‰ for $\delta^2\text{H}$ (Table 2).

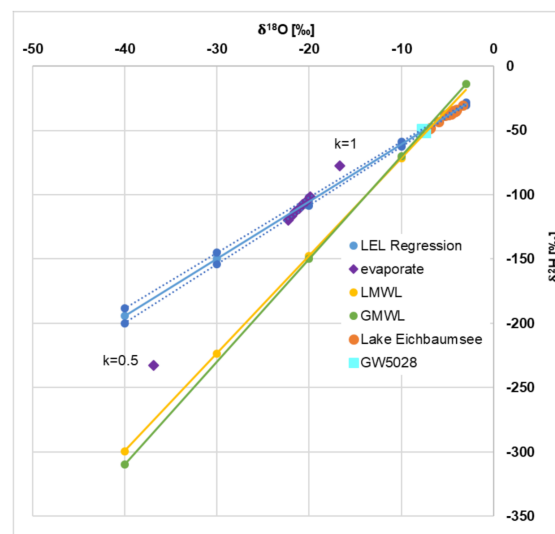


Figure 14. Determination of the isotopic composition of atmospheric moisture. The dotted blue line depicts the 1- σ confidence interval, in which the evaporate signature was allowed to vary by ranging k between 0.86 and 0.92. The extreme evaporation values with $k = 0.5$ (highly seasonal climate) and $k = 1$ (non-seasonal climate) are shown for illustrative purposes. Groundwater well GW5028 marks the intersection between the local evaporation line (LEL) and the LMWL as it exhibits the highest deuterium-excess values. The determination layout of the figure was adapted from Petermann et al. [16].

The surface runoff (S_i) was calculated by projecting the precipitation (P) to the surface runoff area (80,000 m²) bordering the lake, resulting in a surface runoff (S_i) of 2000 m³ in April and 4050 m³ in August. The average isotopic groundwater composition (δ_G : $\delta^{18}\text{O} = -7.07$ ‰; $\delta^2\text{H} = -57.9$ ‰) was determined from wells GW5028 and GW11028, which were sampled in April 2018 and February 2019 (Table 2).

Based on Equation (2) the groundwater discharge (G_i) ranged between 1900 and 4100 m³/d in April and between 2100 and 4800 m³/d in August (Table 2). Lake water exfiltration into the aquifer (G_o) ranged between 1660 and 3800 m³/d in April 2018 and between 1600 and 4200 m³/d in August (Table 2).

From the lake water exfiltration rate (G_o) and the lake water volume a mean water residence time ($\tau = V/G_o$; [16]) of between 1.0 and 2.5 years was calculated for the lake.

It should be noted that the results of the isotopic mass balance presented above are associated with uncertainties and limitations. For instance (and as mentioned earlier), the mass balance model assumes a constant lake volume, which may however change between summer and winter. The isotopic signature of precipitation was derived from Cuxhaven, a location close to the seaside about 100 km away from the study area. Hence, this isotopic signature may not be fully representative of the situation at the lake. The same situation holds for humidity, temperature, and precipitation data that was obtained from a weather station 18 km distance from the lake. Further uncertainties may derive from seasonal and depth-dependent variable isotopic signatures of the groundwater in the hydraulically connected aquifers.

4. Discussion

4.1. Changes in Lake Water Phosphorous Concentrations

The physical and chemical parameters of the lake water column show an annual cycle typical of most temperate lakes with a stratification in spring/summer accompanied by anoxic conditions in the bottom layer, i.e., the hypolimnion, which is characterized by an increase in water phosphorous concentrations with water depth (Figures 3–5). In order to investigate the long-term trend of the phosphorous content of the lake since the last application of Bentophos[®] in autumn 2013 we used the lake monitoring data determined

by local authorities [28,29,40]. This data is based on seasonal water column phosphorous measurements. The lake water phosphorous content was derived by summing the phosphorous content of each water level (i.e., the product of phosphorous concentration in a water depth times the lake water volume at this depth).

Since 2014 there has been a continuous increase of the lake phosphorous content from 226 kg in autumn 2014 to 935 kg in autumn 2019 (Figure 15) which translates to an average increase of ~140 kg/a. This increase has a clear trend with higher increases between the autumns 2014/2015 (309 kg) and 2015/2016 (160 kg) and relative lower ones between the autumns 2016/2017 (68 kg), 2017/2018 (71 kg), and 2018/2019 (61 kg), respectively. The winter lake water circulations which are expected to remove some of the phosphorous from lake waters show no clear trend and remove on average 166 kg/y of phosphorous. The possible phosphorous sources and sinks, as they result from the presented study, are discussed in the following.

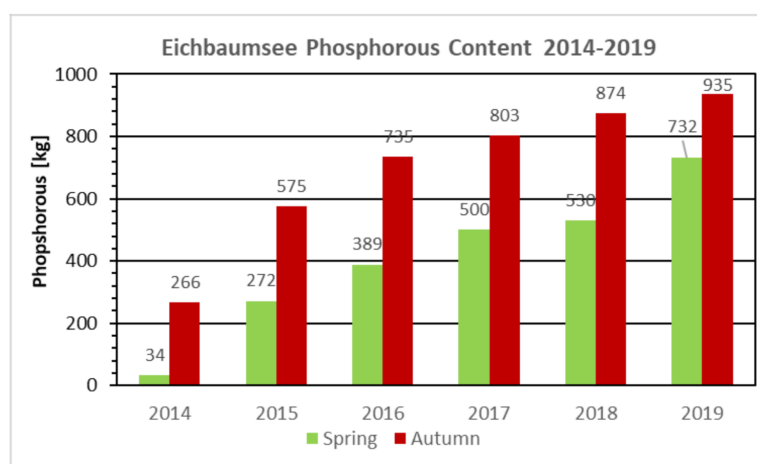


Figure 15. Phosphorous contents of waters in Lake Eichbaumsee between spring 2014 and autumn 2019. Numbers give the phosphorous content in kg. Data are from [28,29,40] and this study.

4.2. Internal Cycling as a Phosphorous Source

Phosphorous removal from the lake water body is believed to be closely related to the precipitation of Fe(III) hydroxides, which scavenge phosphorous from the water column during full lake water oxygenation in winter [41]. In contrast, during anoxic conditions in summer the reverse process of reductive dissolution of Fe(III) hydroxides releases phosphorous from the sediments. Observations from Danish lakes suggest that if surface sediments show a Fe/P ratio of >15 (by weight) the iron pool is high enough to effectively bind phosphorous during aerobic conditions [42]. For instance, in the artificial Lake Hintern Horn, which is located about 3 km southeast of Lake Eichbaumsee, the relatively high sedimentary Fe/P ratio of 17.8 is believed to be the main reason for year-around oligotrophic lake conditions [29]. In Lake Eichbaumsee, in contrast, we observed in surface sediments lower Fe/P ratios (6.40–10.0) (cf. Table S2). These ratios are in the same range as the ratio determined in surface sediments in 2016 (Fe/P = 8.90) [29]. Our observed water column seasonal cycles of iron and manganese follow those of phosphorous (Figures 5 and 6), suggesting an important role of iron and manganese in phosphorous recycling processes. However, a recent study challenges the role of manganese in the removal/liberation processes of phosphorous highlighting the controls of iron redox reactions in phosphorous cycling [43]. Hupfer and Lewandowski [44] pointed out that the retention and mobilization of phosphorous in sediments are very complex processes and dependent on several factors such as the availabilities of oxygen, iron oxides, sulfates/sulfides, carbonates, and phosphorous-binding minerals as well as redox-insensitive binding systems (e.g., Al(OH)₃ and unreducible Fe(III)). In our study no data on the different phosphorous speciations was available, thus these potentially occurring processes could not be investigated in detail. Nevertheless,

it seems that Lake Eichbaumsee sediments retained phosphorous effectively, as sediment phosphorous concentrations increase with decreasing sediment depths, i.e., sediments are a net phosphorous sink (Figure 7). If sediments were to be a net phosphorous source, gradually decreasing sediment phosphorous concentrations towards the sediment surface would be expected, i.e., a pattern similar to that of pore water phosphorous (Figures 7 and 9).

In our study, we observed a diffusive phosphorous flux from sediment pore waters to the lake in February 2019 (i.e., during late winter) with phosphorous flux rates between $0.2 \text{ mg/m}^2/\text{d}$ (E2) and $0.7 \text{ mg/m}^2/\text{d}$ (E4). During this time no oxygen was present in the lowermost water column at location E4 (water depth 16 m) (Figure 4), suggesting that anoxic conditions prevail in the deep water column during winter. At location E2, characterized by a slightly shallower water depth (14 m), oxygen concentrations were constant throughout the water column; however, we still observed a small phosphorous flux from sediments at this location as well. It is possible that diffusive oxygen uptake by sediments, e.g., due to aerobic respiration, may cause steep oxygen gradients close to the sediment/water interface [45], which were not resolved by our water-column sampling. The presented findings indicate that, at least in the deepest parts of the lake, phosphorous is continuously released from the sediments throughout the winter.

Our results of diffusive phosphorous fluxes from sediments are based only on two pore water profiles from two locations representing both summer and winter situations. Thus, it remains unclear how spatially and temporarily representative these results are. Our study did not cover shallower parts of the lake where, e.g., during winter times, presumably phosphorous uptake by sediments will occur (see Section 4.1). Thus, further data is desirable for a more detailed investigation of the seasonal balance of the phosphorous internal cycling in the studied lake. Nevertheless, assuming that the determined phosphorous pore water fluxes are spatially and temporarily representative for the area of the hypolimnion ($154,000 \text{ m}^2$; [28]), the total phosphorous fluxes to the lake range between 128 g/d and 300 g/d in August (48 kg/a and 110 kg/a) and between 32 g/d and 100 g/d in February (11 kg/a and 37 kg/a). These rough estimates show that even under a (unlikely) continuation of the highest phosphorous flux (110 kg/a) throughout a full seasonal cycle this would be not sufficient to fully explain the observed water column phosphorous increase, for instance the phosphorous increase of 344 kg between April and November 2018 (=218 days, i.e., 576 kg/a) (Figure 15).

The observed trend of relatively higher lake water phosphorous increase in the seasons 2014 to 2016 compared to the following years (see Section 4.1) may be explained by a reduced phosphorous release from the sediments after 2016. However, the highest lake water phosphorous increase (relative to the previous year) was observed in summer 2015 (Figure 15), which was after Bentophos[®] phosphorous removal in November 2013. Bentophos[®] is expected to remove and fix phosphorous efficiently [46] and the observed sedimentary phosphorous concentration peaks (corresponding to peaks in lanthanum) most probably reflect this enhanced phosphorous accumulation resulting from the Bentophos[®] applications (Figure 7). It is not likely that this fixed phosphorous was recycled again as the discussed pore water phosphorous concentration profiles do not indicate any additional phosphorous mobilization from these sediment layers characterized by phosphorous and lanthanum concentration peaks (Figures 9 and 11).

In conclusion, the discussions above show that the observed lake water phosphorous increase cannot convincingly be explained phosphorous internal cycling only.

4.3. Groundwater-Borne Phosphorous Flux

As mentioned above, the collected data suggests that according to the water stable isotope mass balance there is an exchange between the aquifer represented by well GW979 and the lake water body. This exchange causes phosphorous flux from the lake to the aquifer and vice versa. Using the range of groundwater exfiltration into the aquifer (G_o) (Table 2) and the average phosphorous concentration of the lake water (0.49 mg/L ; average of November and February) the phosphorous flux to the aquifer ranged between $0.8\text{--}1.1 \text{ kg/d}$.

In contrast, combining the range of the groundwater discharge to the lake (G_i) with the phosphorous concentration of the aquifer groundwater at well GW979 (0.7 mg/L), results in phosphorous fluxes to the lake via groundwater discharge of between 1.3–3.3 kg/d. Thus, the net phosphorous infiltration to the lake amounts to 0.4–1.1 kg/d or 150–390 kg/a. It should be noted that the phosphorous flux calculated based on the water stable isotope balance is a long-term average flux (note, the lake water residence time is ~1 to 2.5 years) and thus does not reflect short-term seasonal changes in the groundwater phosphorous supply. Nevertheless, the isotope mass balance suggests that groundwater discharge to the lake is in the same range or higher than the sediment-derived phosphorous flux.

The observed trend of a lower total phosphorous increase in the lake water in autumn since 2016 (see Section 4.1) can be explained by the difference between lake water and groundwater phosphorous concentrations. The difference of the lake water to the groundwater concentration of 0.70 mg/L was highest in springs 2014 and 2015 (lake phosphorous ~0.15 mg/L) and was less in spring 2019 (~0.43 mg/L). With decreasing differences in the phosphorous concentrations between the two water bodies one expects the phosphorous increase in Lake Eichbaumsee to reach a plateau value.

Without any direct observations or direct measurements of phosphorous-rich groundwater discharge to the lake, it is difficult to exactly define the origin of phosphorous in the lake. Groundwater, while seeping through lake sediments, may mobilize phosphorous from iron oxides, phosphorous-bearing minerals, and organic matter buried in lake sediments [10,13]. Although phosphorous was long considered to be immobile in groundwater, there is increasing evidence that the eutrophication of lakes is driven by groundwater discharge rich in phosphorous and that this may be an important albeit so far neglected source [47–51]. For instance, studies of the eutrophic Lake Arendsee (Germany) revealed that groundwater discharge was responsible for more than 50% of the total phosphorous supply to the lake [48]. The importance of groundwater-borne phosphorous may also hold for oligotroph lakes [49].

Phosphorous in groundwater may derive from natural and anthropogenic sources [52,53]. In the presented study, phosphorous groundwater concentrations are below the EU drinking water standard (2.20 mg P L⁻¹), thus there is no indication of any substantial impact of anthropogenic phosphorous sources. Identifying such sources is challenging, and analyses of the phosphorous oxygen isotope composition may be a powerful tool to be used in further studies on the lake phosphorous cycle [54].

5. Conclusions

More than 70% of the lakes in Germany ($n = 732$) do not achieve the “good ecological status” required by the European Water Framework Directive [55,56], with excess nutrient loads being the major cause for the deterioration of the quality of lake waters. Thus, there is a general need for restoration measures which are concentrated on the internal phosphorous cycle only. The presented study was carried out at the eutrophic Lake Eichbaumsee, which is characterized by poor water quality caused by high phosphorous concentrations. Despite several remediation attempts, e.g., water aeration or removal of dissolved phosphorous by co-precipitation with aluminum sulfate and lanthanum-modified bentonite (Bentophos[®]), lake water phosphorous concentrations have increased significantly over the years. Assuming that our determined sediment pore water fluxes (11–110 kg/a) are temporally and spatially representative, the lake internal phosphorous source (i.e., phosphorous released from sediments) is not sufficient to explain the observed long-term phosphorous increase in the water column. Furthermore, the results do not indicate any remobilization of sedimentary phosphorous co-precipitated with Bentophos[®]. Based on a D/O mass balance we show that groundwater-borne phosphorous flux is a significant but so far not considered phosphorous source for the water body of Lake Eichbaumsee. This groundwater source needs to be considered in any successful remediation attempts of the lake, a situation which is most probably also relevant for other eutrophic groundwater-fed lakes.

Supplementary Materials: The following are available online at <https://www.mdpi.com/2073-4441/13/4/563/s1>, Table S1: Chemical composition of groundwater, Table S2: Chemical composition of sediments (n.d. = not determined; b.d. = below detection).

Author Contributions: Conceptualization, J.C.S., M.S. and S.C.W.; data curation: W.F., N.C., M.L., U.R. and S.C.W.; methodology: W.F., J.C.S., M.S., K.K., M.L. J.-H.R., U.R., N.C., I.Z. and S.C.W.; Project administration: J.C.S., U.R., S.C.W.; Writing—original draft: W.F., J.C.S., M.S., J.-H.R. and S.C.W.; review and editing, J.C.S., M.S., M.L., N.C., U.R. and S.C.W. All authors have read and agreed to the published version of the manuscript.

Funding: This research received no external funding.

Institutional Review Board Statement: Not applicable.

Informed Consent Statement: Not applicable.

Acknowledgments: We thank the scientific diving team of the Institute of Geoscience (Kiel University) for their support in collecting the sediments cores. We are grateful for the support of S. Schäfer-Gomm (Behörde für Umwelt, Klima, Energie und Agrarwirtschaft, Hamburg) and P. Seidel (Bezirksamt Bergedorf). The constructive comments made by two anonymous referees are gratefully acknowledged.

Conflicts of Interest: The authors declare no conflict of interest.

References

1. Ho, J.C.; Michalak, A.M.; Pahlevan, N. Widespread global increase in intense lake phytoplankton blooms since the 1980s. *Nat. Cell Biol.* **2019**, *574*, 667–670. [[CrossRef](#)] [[PubMed](#)]
2. Michalak, A.M.; Anderson, E.J.; Beletsky, D.; Boland, S.; Bosch, N.S.; Bridgeman, T.B.; Chaffin, J.D.; Cho, K.; Confesor, R.; Daloğlu, I.; et al. Record-setting algal bloom in Lake Erie caused by agricultural and meteorological trends consistent with expected future conditions. *Proc. Natl. Acad. Sci. USA* **2013**, *110*, 6448–6452. [[CrossRef](#)]
3. Beaulieu, M.; Pick, F.R.; Gregory-Eaves, I. Nutrients and water temperature are significant predictors of cyanobacterial biomass in a 1147 lakes data set. *Limnol. Oceanogr.* **2013**, *58*, 1736–1746. [[CrossRef](#)]
4. Conley, D.J.; Paerl, H.W.; Howarth, R.W.; Boesch, D.F.; Seitzinger, S.P.; Havens, K.E.; Lancelot, C.; Likens, G.E. Ecology: Controlling eutrophication: Nitrogen and phosphorus. *Science* **2009**, *323*, 1014–1015. [[CrossRef](#)] [[PubMed](#)]
5. Søndergaard, M.; Jensen, J.P.; Jeppesen, E. Seasonal response of nutrients to reduced phosphorus loading in 12 Danish lakes. *Freshw. Biol.* **2005**, *50*, 1605–1615. [[CrossRef](#)]
6. Magnuson, J.J.; Kratz, T.K.; Benson, B.J. *Long-Term-Dynamics of Lakes in the Landscape-Long-Term Ecological Research on North Temperate Lakes*; Oxford University Press: Oxford, UK, 2006; 464p.
7. Welch, E.B.; Jacoby, J.M. On determining the principal source of phosphorus causing summer algal blooms in Western Washington Lakes. *Lake Reserv. Manag.* **2001**, *17*, 55–65. [[CrossRef](#)]
8. Beutel, M.W.; Horne, A.J. Nutrient fluxes from profundal sediment of ultra-oligotrophic Lake Tahoe, California/Nevada: Implications for water quality and management in a changing climate. *Water Resour. Res.* **2018**, *54*, 1549–1559. [[CrossRef](#)]
9. Rosenberry, D.O.; Winter, T.C.; Likens, G.E. *Hydrologic Processes and the Water Budget*; University of California Press: Berkeley, CA, USA, 2009; pp. 22–68.
10. Lewandowski, J.; Meinikmann, K.; Nützmann, G.; Rosenberry, D.O. Groundwater—The disregarded component in lake water and nutrient budgets. Part 2: Effects of groundwater on nutrients. *Hydrol. Process.* **2015**, *29*, 2922–2955. [[CrossRef](#)]
11. Rosenberry, D.O.; Lewandowski, J.; Meinikmann, K.; Nützmann, G. Groundwater—The disregarded component in lake water and nutrient budgets. Part 1: Effects of groundwater on hydrology. *Hydrol. Process.* **2015**, *29*, 2895–2921. [[CrossRef](#)]
12. Stachelek, J.; Soranno, P.A. Does freshwater connectivity influence phosphorus retention in lakes? *Limnol. Oceanogr.* **2019**, *64*, 1586–1599. [[CrossRef](#)]
13. Kazmierczak, J.; Postma, D.; Müller, S.; Jessen, S.; Nilsson, B.; Czekaj, J.; Engesgaard, P. Groundwater-controlled phosphorus release and transport from sandy aquifer into lake. *Limnol. Oceanogr.* **2020**, *65*, 2188–2204. [[CrossRef](#)]
14. Arnoux, M.; Barbecot, F.; Gibert-Brunet, E.; Gibson, J.; Rosa, E.; Noret, A.; Monvoisin, G. Geochemical and isotopic mass balances of kettle lakes in southern Quebec (Canada) as tools to document variations in groundwater quantity and quality. *Environ. Earth Sci.* **2017**, *76*, 106. [[CrossRef](#)]
15. Gibson, J.; Birks, S.; Yi, Y. Stable isotope mass balance of lakes: A contemporary perspective. *Quat. Sci. Rev.* **2016**, *131*, 316–328. [[CrossRef](#)]
16. Petermann, E.; Gibson, J.J.; Knöller, K.; Pannier, T.; Weiß, H.; Schubert, M. Determination of groundwater discharge rates and water residence time of groundwater-fed lakes by stable isotopes of water (^{18}O , ^2H) and radon (^{222}Rn) mass balances. *Hydrol. Process.* **2018**, *32*, 805–816. [[CrossRef](#)]
17. Knöller, K.; Strauch, G. The application of stable isotopes for assessing the hydrological, sulfur, and iron balances of acidic mining lake ML 111 (Lusatia, Germany) as a basis for biotechnological remediation. *Water Air Soil Pollut. Focus* **2002**, *2*, 3–14. [[CrossRef](#)]

18. Janssen, A.B.; van Wijk, D.; van Gerven, L.P.; Bakker, E.S.; Brederveld, R.J.; DeAngelis, D.L.; Janse, J.H.; Mooij, W.M. Success of lake restoration depends on spatial aspects of nutrient loading and hydrology. *Sci. Total Environ.* **2019**, *679*, 248–259. [[CrossRef](#)]
19. Jeppesen, E.; Søndergaard, M.; Jensen, J.P.; Havens, K.E.; Anneville, O.; Carvalho, L.; Coveney, M.F.; Deneke, R.; Dokulil, M.T.; Foy, B.; et al. Lake responses to reduced nutrient loading—An analysis of contemporary long-term data from 35 case studies. *Freshw. Biol.* **2005**, *50*, 1747–1771. [[CrossRef](#)]
20. Schindler, D.W.; Hecky, R.E.; Findlay, D.L.; Stainton, M.P.; Parker, B.R.; Paterson, M.J.; Beaty, K.G.; Lyng, M.; Kasian, S.E.M. Eutrophication of lakes cannot be controlled by reducing nitrogen input: Results of a 37-year whole-ecosystem experiment. *Proc. Natl. Acad. Sci. USA* **2008**, *105*, 11254–11258. [[CrossRef](#)]
21. Nöges, T.; Laugaste, R.; Nöges, P.; Tönno, I. Critical N:P ratio for cyanobacteria and N₂-fixing species in the large shallow temperate lakes Peipsi and Võrtsjärv, North-East Europe. *Hydrobiology* **2008**, *599*, 77–86. [[CrossRef](#)]
22. Rohrlack, T.; Dittmann, E.; Henning, M.; Börner, T.; Kohl, J.G. Role of microcystins in poisoning and food ingestion inhibition of *Daphnia galeata* caused by the cyanobacterium *Microcystis aeruginosa*. *Appl. Environ. Microbiol.* **1999**, *65*, 737–739. [[CrossRef](#)]
23. Peterson, S.A. Lake restoration by sediment removal. *JAWRA J. Am. Water Resour. Assoc.* **1982**, *18*, 423–436. [[CrossRef](#)]
24. Galvez-Cloutier, R.; Saminathan, S.K.M.; Boillot, C.; Triffaut-Bouchet, G.; Bourget, A.; Soumis-Dugas, G. An evaluation of several in-lake restoration techniques to improve the water quality problem (eutrophication) of Saint-Augustin Lake, Quebec, Canada. *Environ. Manag.* **2012**, *49*, 1037–1053. [[CrossRef](#)]
25. Reitzel, K.; Hansen, J.; Andersen, F.Ø.; Hansen, K.S.; Jensen, H.S. Lake restoration by dosing aluminum relative to mobile phosphorus in the sediment. *Environ. Sci. Technol.* **2005**, *39*, 4134–4140. [[CrossRef](#)] [[PubMed](#)]
26. Copetti, D.; Finsterle, K.; Marziali, L.; Stefani, F.; Tartari, G.; Douglas, G.; Reitzel, K.; Spears, B.M.; Winfield, I.J.; Crosa, G.; et al. Eutrophication management in surface waters using lanthanum modified bentonite: A review. *Water Res.* **2016**, *97*, 162–174. [[CrossRef](#)] [[PubMed](#)]
27. Egemose, S.; Wauer, G.; Kleeberg, A. Resuspension behaviour of aluminium treated lake sediments: Effects of ageing and pH. *Hydrobiology* **2009**, *636*, 203–217. [[CrossRef](#)]
28. Spieker, J.; Göring, H. *Gewässerökologisches Monitoringprogramm 2015. Gutachten im Auftrag der Freien und Hansestadt Hamburg; Behörde für Stadtentwicklung und Umwelt, Amt für Umweltschutz, Gewässerschutz.*—Hrsg.: (Konzepte Lösungen Sanierungen im Gewässerschutz); Planungsbüro für Gewässerschutz: Hamburg, Germany, 2016.
29. Spieker, J.; Göring, H. *See Hinterm Horn—Eichbaumsee: Vergleichende Untersuchungen zum Eisen-Phosphor-Kreislauf. Gutachten im Auftrag der Freien und Hansestadt Hamburg; Behörde für Stadtentwicklung und Umwelt, Amt für Umweltschutz, Gewässerschutz.*—Hrsg.: Konzepte Lösungen Sanierungen im Gewässerschutz—Planungsbüro für Gewässerschutz: Hamburg, Germany, 2017.
30. Seeberg-Elverfeldt, J.; Schlüter, M.; Feseker, T.; Kölling, M. Rhizon sampling of porewaters near the sediment-water interface of aquatic systems. *Limnol. Oceanogr. Methods* **2005**, *3*, 361–371. [[CrossRef](#)]
31. Charette, M.A.; Allen, M.C. Precision Ground Water Sampling in Coastal Aquifers Using a Direct-Push, Shielded-Screen Well-Point System. *Ground Water Monit. Remediat.* **2006**, *26*, 87–93. [[CrossRef](#)]
32. Fick, A. Über Diffusion. *Ann. Phys.* **1855**, *170*, 59–86. [[CrossRef](#)]
33. Ullman, W.J.; Aller, R.C. Diffusion coefficients in nearshore marine sediments. *Limnol. Oceanogr.* **1982**, *27*, 552–556. [[CrossRef](#)]
34. Craig, H.; Gordon, L.I. Deuterium and oxygen-18 variations in the ocean and the marine atmosphere. In *Proceedings of the Conference on Stable Isotopes in Oceanographic, Studies Paleotemperatures, Spoleto, Italy*; Tongiorgi, E., Ed.; Consiglio Nazionale delle Ricerche, Laboratorio de Geologia Nucleare: Pisa, Italy, 1965; pp. 9–130.
35. Horita, J.; Wesolowski, D.J. Liquid-vapor fractionation of oxygen and hydrogen isotopes of water from the freezing to the critical temperature. *Geochim. Cosmochim. Acta* **1994**, *58*, 3425–3437. [[CrossRef](#)]
36. Gonfiantini, R. Chapter 3—Environmental isotopes in lake studies. In *The Terrestrial Environment*; Fritz, B.P., Fontes, J.C., Eds.; Elsevier: Amsterdam, The Netherlands, 1986; pp. 113–168.
37. Dinçer, T. The use of oxygen 18 and deuterium concentrations in the water balance of lakes. *Water Resour. Res.* **1968**, *4*, 1289–1306. [[CrossRef](#)]
38. Zuber, A. On the environmental isotope method for determining the water balance components of some lakes. *J. Hydrol.* **1983**, *61*, 409–427. [[CrossRef](#)]
39. Craig, H. Isotopic variations in meteoric waters. *Science* **1961**, *133*, 1702–1703. [[CrossRef](#)]
40. Seiler, C.; Redelstein, R. *Bericht zum Monitoring des Eichbaumsees im Jahr 2019; Gutachten im Auftrag der Freien und Hansestadt Hamburg, Institut für Hygiene und Umwelt: Hamburg, Germany, 2020.*
41. Amirbahman, A.; Pearce, A.R.; Bouchard, R.J.; Norton, S.A.; Steven Kahl, J. Relationship between hypolimnetic phosphorus and iron release from eleven lakes in Maine, USA. *Biogeochemistry* **2003**, *65*, 369–386. [[CrossRef](#)]
42. Jensen, H.S.; Kristensen, P.; Jeppesen, E.; Skytthe, A. Iron:phosphorus ratio in surface sediment as an indicator of phosphate release from aerobic sediments in shallow lakes. *Hydrobiologia* **1992**, *235*, 731–743. [[CrossRef](#)]
43. Chen, M.; Ding, S.; Wu, Y.; Fan, X.; Jin, Z.; Tsang, D.C.; Wang, Y.; Zhang, C. Phosphorus mobilization in lake sediments: Experimental evidence of strong control by iron and negligible influences of manganese redox reactions. *Environ. Pollut.* **2019**, *246*, 472–481. [[CrossRef](#)]
44. Hupfer, M.; Lewandowski, J. Oxygen controls the phosphorus release from lake sediments—A long-lasting paradigm in Limnology. *Int. Rev. Hydrobiol.* **2008**, *93*, 415–432. [[CrossRef](#)]

45. Schwefel, R.; Steinsberger, T.; Bouffard, D.; Bryant, L.D.; Müller, B.; Wüest, A. Using small-scale measurements to estimate hypolimnetic oxygen depletion in a deep lake. *Limnol. Oceanogr.* **2017**, *63*, S54–S67. [[CrossRef](#)]
46. Epe, T.S.; Finsterle, K.; Yasseri, S. Nine years of phosphorus management with lanthanum modified bentonite (Phoslock) in a eutrophic, shallow swimming lake in Germany. *Lake Reserv. Manag.* **2017**, *33*, 119–129. [[CrossRef](#)]
47. US Geological Survey. 2014. Available online: https://toxics.usgs.gov/highlights/phosphorous_migration.html (accessed on 26 October 2020).
48. Meinikmann, K.; Hupfer, M.; Lewandowski, J. Phosphorus in groundwater discharge—A potential source for lake eutrophication. *J. Hydrol.* **2015**, *524*, 214–226. [[CrossRef](#)]
49. Ommen, D.A.O.; Kidmose, J.; Karan, S.; Flindt, M.R.; Engesgaard, P.; Nilsson, B.; Andersen, F. Østergaard Importance of groundwater and macrophytes for the nutrient balance at oligotrophic Lake Hampen, Denmark. *Ecohydrology* **2011**, *5*, 286–296. [[CrossRef](#)]
50. Holman, I.P.; Whelan, M.J.; Howden, N.J.K.; Bellamy, P.H.; Willby, N.J.; Rivas-Casado, M.; McConvey, P.J. Phosphorus in groundwater—an overlooked contributor to eutrophication? *Hydrol. Process.* **2008**, *22*, 5121–5127. [[CrossRef](#)]
51. Jarosiewicz, A.; Witek, Z. Where do nutrients in an inlet-less lake come from? The water and nutrient balance of a small mesotrophic lake. *Hydrobiol.* **2014**, *724*, 157–173. [[CrossRef](#)]
52. Heathwaite, A.; Dils, R. Characterising phosphorus loss in surface and subsurface hydrological pathways. *Sci. Total Environ.* **2000**, *251–252*, 523–538. [[CrossRef](#)]
53. Holman, I.; Howden, N.; Bellamy, P.; Willby, N.; Whelan, M.; Casado, M.R. An assessment of the risk to surface water ecosystems of groundwater P in the UK and Ireland. *Sci. Total Environ.* **2010**, *408*, 1847–1857. [[CrossRef](#)] [[PubMed](#)]
54. Nisbeth, C.S.; Tamburini, F.; Kidmose, J.; Jessen, S.; O’Connell, D.W. Analysis of oxygen isotopes of inorganic phosphate ($\delta^{18}\text{O}_\text{P}$) in freshwater: A detailed method description. *Hydrol. Earth Syst. Sci. Discuss.* **2019**, *2019*, 1–18.
55. Rucker, J.; Nixdorf, B.; Quiel, K.; Grüneberg, B. North German Lowland Lakes Miss Ecological Water Quality Standards—A Lake Type Specific Analysis. *Water* **2019**, *11*, 2547. [[CrossRef](#)]
56. Bundesministerium für Umwelt und Bau/Umweltbundesamt (BMUB/UBA). Water Framework Directive—The Status of German Waters 2015; BMU/UBA: Bonn/Dessau, Germany. 2016. Available online: https://www.gewaesser-bewertung.de/files/wrrl_englische_version_dez_2016.pdf (accessed on 1 December 2020).